Contents lists available at ScienceDirect

# Nuclear Inst. and Methods in Physics Research, A

journal homepage: www.elsevier.com/locate/nima

# Influence of radiation damage on the absorption of near-infrared light in silicon

C. Scharf *, F. Feindt, R. Klanner

*Institute for Experimental Physics, University of Hamburg, Luruper Chaussee 147, D 22761, Hamburg, Germany*

## ARTICLE INFO

## ABSTRACT

The absorption length, $\lambda_{abs}$, of light with wavelengths between 0.95 and 1.30 μm in silicon irradiated with 24 GeV/c protons to 1 MeV neutron equivalent fluences up to $8.6 \times 10^{15}$ cm$^{-2}$ has been measured. It is found that $\lambda_{abs}$ decreases with fluence due to radiation-induced defects. A phenomenological parametrization of the radiation-induced change of $\lambda_{abs}$ as a function of wavelength and neutron equivalent fluence at room temperature is given. The observation of the decrease of $\lambda_{abs}$ with irradiation is confirmed by edge-TCT measurements on irradiated silicon strip detectors. Using the measured wavelength dependence of $\lambda_{abs}$, the change of the silicon band-gap with fluence is determined.

## 1. Introduction

A standard way of determining the Charge-Collection-Efficiency, $CCE$, of radiation-damaged silicon sensors uses red and near-infrared (NIR) light to generate electron–hole pairs. In order to determine the absolute number of produced charge carriers, the light-absorption length, $\lambda_{abs}$, has to be known. Radiation produces defect states in the silicon band-gap, which are expected to cause a reduction of $\lambda_{abs}$.

In Ref. [1] the photo-conductivity of silicon for wavelengths up to $\lambda = 3$ μm has been measured before and after irradiation. Before irradiation no photo-conductivity has been observed. After irradiation it becomes significant. The results have been described by an irradiation-induced reduction of the silicon band-gap by up to 100 meV. However, the fluences of these studies are significantly higher than the ones investigated in this paper, for which a band-gap narrowing of only a few meV is expected.

In this work the transmittance of high-ohmic n-doped silicon irradiated with 24 GeV/c protons up to 1 MeV neutron equivalent fluences, $\Phi_{eq}$, of $8.6 \times 10^{15}$ cm$^{-2}$ for light with $\lambda$ between 0.95 and 1.30 μm has been measured. From the results $\lambda_{abs}(\Phi_{eq}, \lambda)$ is derived and the inverse of the radiation-induced absorption length

$$\alpha_{irr}(T, \Phi_{eq}, \lambda) = 1/\lambda_{abs}(T, \Phi_{eq}, \lambda) - 1/\lambda_{abs}(T, 0, \lambda) \quad (1)$$

determined. The observed decrease of $\lambda_{abs}$ with $\Phi_{eq}$ is confirmed by edge-TCT measurement using light from a sub-nanosecond laser with $\lambda = 1.052$ μm [2,3]. The measured dependence of $\lambda_{abs}$ on $\Phi_{eq}$ is also used to investigate a possible narrowing of the silicon energy band-gap, $E_{gap}$, with $\Phi_{eq}$.

## 2. Samples and light-absorption measurements

Four samples of phosphorus-doped silicon with $\approx 3.5$ kΩ cm resistivity and $\approx 300$ μm thickness were irradiated with 24 GeV/c protons to $\Phi_{eq} = (2.4, 4.9, 6.4, 8.6) \times 10^{15}$ cm$^{-2}$ at the CERN PS. The uncertainty of the fluence is about ±10%. For the calculation of $\Phi_{eq}$ a hardness factor $\kappa = 0.62$ is used [4]. After irradiation, the samples were stored in a freezer, being only warmed up to room temperature for the measurements; these were performed at $20\pm2$ °C. A fifth sample, which was not irradiated, provided the results for non-irradiated silicon. The crystals were bare and the thickness of the naturally grown SiO$_2$ layer is much smaller than the wavelength of the light used for the transmission measurements. The mechanical thicknesses of the silicon pieces were measured using a caliper to an accuracy of 2 μm.

The transmittance measurements were performed using an Agilent CARY 5000 UV–VIS–NIR spectro-photometer [5]. Fig. 1 shows the results. The transmittance, $Tr$, is close to zero at $\lambda = 0.95$ μm and increases to $\approx 50\%$ at $\lambda = 1.30$ μm. $Tr$ decreases smoothly with $\Phi_{eq}$. From repeated transmittance measurements of the non-irradiated samples a reproducibility of the results at the 0.1% level for $\lambda \geq 1.05$ μm is deduced. For $\lambda < 1.05$ μm, $Tr$ has a strong temperature dependence and the reproducibility worsens to $\approx 1\%$.

Next, the transmittance measurements are compared to the expectations from literature values. Refs. [6,7] give tables of $n(\lambda)$ and $1/\lambda_{abs}(\lambda)$ and their temperature dependencies at 300 K. The transmittance, $Tr(\lambda)$, of an optical material of thickness $d$, index of refraction $n(\lambda)$ and absorption length $\lambda_{abs}(\lambda)$ is given by

$$Tr(n, \lambda_{abs}, d) = \frac{Tra^2 \cdot e^{-d/\lambda_{abs}}}{1 - \left(Ref \cdot e^{-d/\lambda_{abs}}\right)^2}, \quad (2)$$

* Correspondence to: Institut für Physik, Humboldt-Universität zu Berlin, Newtonstr. 15, D 12489 Berlin, Germany.
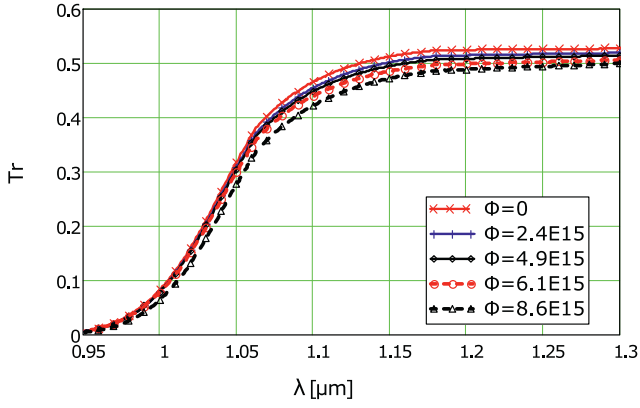 *E-mail address:* Christian.Scharf@desy.de (C. Scharf).

**Fig. 1.** Measured transmittance as a function of wavelength, $\lambda$, for different 1 MeV equivalent neutron fluences, $\Phi_{eq}$, in units of cm$^{-2}$.
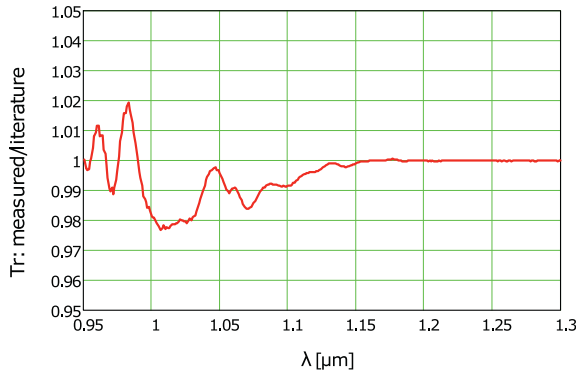


**Fig. 2.** Ratio of the measured transmittance, $Tr(\lambda)$, to the literature values at +20 °C for the non-irradiated silicon.



**Fig. 3.** Measured $\lambda_{abs}$ as a function of $\lambda$ for the different $\Phi_{eq}$-values, and comparison to the values from Ref. [6] for non-irradiated silicon.



**Fig. 4.** $\alpha_{irr}$ as a function of $\Phi_{eq}$ for selected wavelengths. Within the experimental uncertainties $\alpha_{irr}(\Phi_{eq})$ is proportional to $\Phi_{eq}$.

with the relations for the transmittance, $Tra(\lambda)$, and reflectivity, $Ref(\lambda)$, of a single air-silicon interface

$$Ref(\lambda) = \frac{(n(\lambda)-1)^2}{(n(\lambda)+1)^2} \quad \text{and} \quad Tra(\lambda) = 1 - Ref(\lambda) = \frac{4 \cdot n(\lambda)}{(n(\lambda)+1)^2}. \quad (3)$$

These are the Fresnel formulae for normal light incidence between a medium of refractive index 1 (air) and $n$ (silicon). To derive Eq. (2), multiple transmissions and reflections at both air-silicon interfaces have to be considered. This results in a geometrical series which, in the limit an infinite number of reflections, gives Eq. (2).

Fig. 2 shows for the non-irradiated silicon the ratio of the measured to the expected transmittance at 20 °C, after the following corrections: The $\lambda$-scale is shifted by $-1.0$ nm and the transmittance scaled by 0.4%, which is within the calibration uncertainty of the photospectrometer. With these corrections, the maximum difference is below $\pm3\%$. Without them, the difference is +15% at $\lambda = 0.95$ μm, illustrating the high sensitivity of the results to the $\lambda$-scale at short wavelengths.

## 3. Results

From Eq. (2) the dependence of $\lambda_{abs}$ on $Tr$ can be derived:

$$\lambda_{abs}(\lambda) = \frac{d}{\ln\left(\frac{Tra(\lambda)^2 + \sqrt{Tra(\lambda)^4 + 4 \cdot Ref(\lambda)^2 \cdot Tra(\lambda)^2}}{2 \cdot Tr(\lambda)}\right)}. \quad (4)$$

Fig. 3 shows the experimental results for $\lambda_{abs}(\lambda)$ for the different $\Phi_{eq}$-values, using $n(\lambda)$ at 20 °C from Ref. [6] for both irradiated and non-irradiated silicon. In addition, the values for $\lambda_{abs}$ at 20 °C from Ref. [6] are shown. The results for the non-irradiated sensor agree with
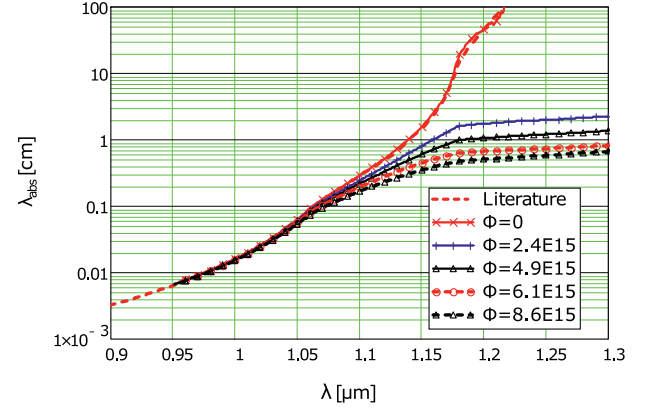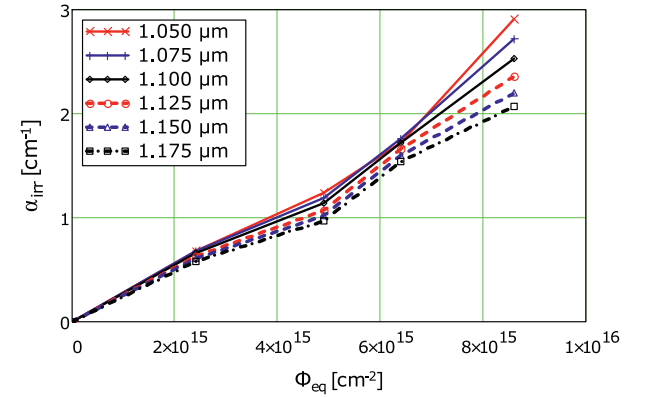
the literature values up to $\lambda = 1.25$ μm. For higher values they deviate. Note that at $\lambda = 1.2$ μm, $\lambda_{abs} \approx 50$ cm, which is much larger than the sample thickness of 0.03 cm, and the determination of $\lambda_{abs}$ becomes unreliable. For the irradiated silicon $\lambda_{abs}$ decreases with $\Phi_{eq}$.

The inverse of the radiation-induced absorption length, $\alpha_{irr}$, has been introduced in Eq. (1). Fig. 4 shows the experimental results for $\alpha_{irr}(\Phi)$ for selected values of $\lambda$. It is observed that $\alpha_{irr}(\Phi_{eq})$ is approximately proportional to $\Phi_{eq}$. Fig. 3 shows that $\lambda_{abs}$ rapidly decreases with decreasing $\lambda$, and that for small $\lambda$ values, $\alpha_{irr}$ is the difference of two large numbers. As a result, the determination of $\alpha_{irr}$ is very sensitive to the $\lambda$ calibration of the spectrophotometer for $\lambda \lesssim 1.05$ μm. Given these uncertainties, only results for $\lambda \geq 1.05$ μm are shown in the following.

The proportionality constants, $\alpha_{irr}/\Phi_{eq}$, are obtained by calculating the mean $\alpha_{irr}(\lambda, \Phi_{eq})/\Phi_{eq}$ for every $\lambda$-value. Fig. 5 shows the results for $\lambda = 1.05$ to 1.30 μm. The error bars reflect the uncertainty obtained from the straight-line fits to $\alpha_{irr}(\Phi_{eq})$. Other sources of uncertainties considered are: 1% for $n$, 2% for $Tr$, 2 μm for the sensor thickness, and 10% for the uncertainty of $\Phi_{eq}$. The latter one, which is the same for all wavelengths, dominates. The results of a fit by a second order polynomial to the data are given in Table 1. The parameters can be used to calculate $\alpha_{irr}(\Phi_{eq}, \lambda)$, and together with Eq. (1) and the values of $\lambda_{abs}(0, \lambda)$ from Ref. [7], the values of $\lambda_{abs}(\Phi_{eq}, \lambda)$. With the assumption that the number of electron–hole pairs is proportional to the light absorption, the number of charge carriers generated by light in radiation-damaged silicon at 20 °C can be obtained.
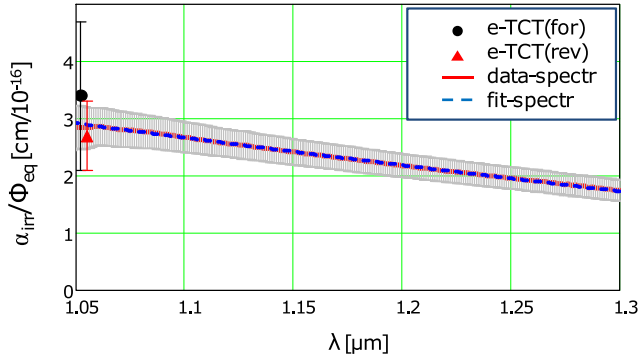
**Fig. 5.** Results for $\alpha_{irr}/\Phi_{eq}$: The edge-TCT results for $\lambda = 1.052$ μm and $-30$ °C are denoted *e-TCT (for)* and *e-TCT (rev)* for forward and reverse voltages, respectively. The photospectrometer data at $+20$ °C are labeled *data-spectr*, and the second-order polynomial fit *fit-spectr*. For clarity the *e-TCT* results are drawn at different $\lambda$ values.

**Table 1**
Results of the second-order polynomial fit $\alpha_{irr}/\Phi_{eq} = a + b \cdot (\lambda - \lambda_0) + c \cdot (\lambda - \lambda_0)^2$ to the data shown in Fig. 5, with the value $\lambda_0 = 1.15$ μm. The first error of $a$ is the statistical uncertainty, the second an estimate of the systematic uncertainty of the analysis method, and the third the result of other systematic effects, which are discussed in the text.

| $a$ [cm] | $b$ [cm/μm] | $c$ [cm/μm²] |
|---|---|---|
| $(2.427 \pm 0.001 \pm 0.4 \pm 0.2) \times 10^{-16}$ | $(4.805 \pm 0.005) \times 10^{-16}$ | $(1.29 \pm 0.02) \times 10^{-16}$ |

## 4. Comparison to edge-TCT results

In Ref. [2,3] the edge-TCT (Transient-Current-Technique) is used to measure $\lambda_{abs}(\Phi_{eq})$ for proton fluences, $\Phi_{eq}$, between 0 and $13 \times 10^{15}$ cm$^{-2}$. For edge-TCT [8], focused light from a sub-nanosecond laser is injected through a polished edge into a strip sensor parallel to the surface and perpendicular to the strips, and the current transients are recorded. By moving the beam normal to the sensor surface, the charge-collection efficiency and the electric field as a function of depth, $x$, can be determined [9]. AC-coupled strip detectors with an active thickness of 285 μm and a strip pitch of 80 μm built on $\approx 5$ kΩ cm $n$-doped silicon were investigated. The fourth strip, located 1350 μm from the sensor edge, and the ninth strip, located $L = 400$ μm from the first strip, were read out. The absorption length is obtained from the integral of the current of the first strip, $Q_1$, and of the second readout strip, $Q_2$, using the relation $\lambda_{abs} = L/\ln(Q_1/Q_2)$.

The wavelength of the laser light was $\lambda = 1.052$ μm. Because of high leakage currents, the measurements were performed at $-30$ °C. The irradiated sensors were biased with forward voltages, $V_{forw}$, as well as with reverse voltages, $V_{rev}$, between 0 and 1000 V. A constant charge ratio, $Q_1(x)/Q_2(x)$, as a function of $x$ was expected. However, because of a number of experimental problems, this was not the case [2,3]. The analysis is performed in the $x$-region, where $Q_1/Q_2$ is approximately constant.

It is found that $\alpha_{irr} \propto \Phi_{eq}$, as was already observed for the spectrophotometer measurements. The results for the sensor irradiated to $\Phi_{eq} = 9.4 \times 10^{15}$ cm$^{-2}$ are: For $V_{forw}$ between 500 and 1000 V the value found for $\alpha_{irr}/\Phi_{eq}$ is $(2.7 \pm 0.6) \times 10^{-16}$ cm, and for $V_{rev}$ between 500 and 1000 V, $(3.4 \pm 1.3) \times 10^{-16}$ cm. The large uncertainties reflect the observed increase of $\alpha_{irr}$ with voltage. As shown in Fig. 5, the results are compatible with the value $(2.9 \pm 0.4) \times 10^{-16}$ cm determined from the spectrophotometer measurements at $+20$ °C. These results confirm the reduction of $\lambda_{abs}$ due to radiation damage.

## 5. Discussion of the results

The attenuation of radiation in matter as a function of the path-length $x$ follows an exponential law $e^{-\alpha \cdot x}$, with $\alpha = \sum_i (N_i \cdot \sigma_i)$,
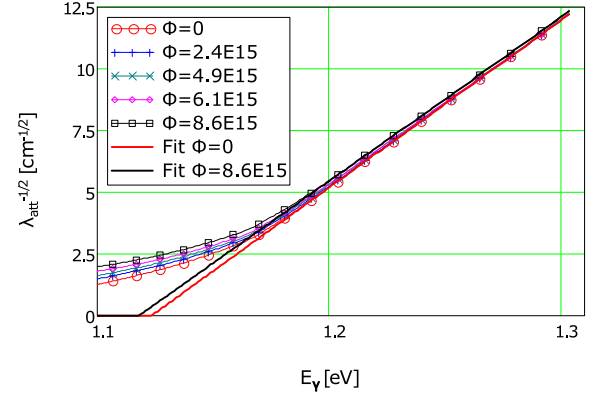


**Fig. 6.** Plot of $\sqrt{1/\lambda_{abs}}$ as a function of $E_\gamma$ for the different $\Phi_{eq}$-values. Straight-line fits in the range $E_\gamma = 1.2$–1.3 eV are shown, which allow to determine $E_g$ as a function of $\Phi_{eq}$.

where $N_i$ is the density of scattering centers and $\sigma_i$ the corresponding cross-sections. Analogously one can define

$$\alpha_{irr}(\Phi_{eq}) = \sum_i \left( N_i(\Phi_{eq}) \cdot \sigma_i(\lambda) \right) = \Phi_{eq} \cdot \sum_i \left( \beta_i \cdot \sigma_i(\lambda) \right). \quad (5)$$

The right-hand side of the equation uses the experimental observation of Section 3 that $\alpha_{irr} \propto \Phi_{eq}$, which allows introducing the introduction rates $\beta_i = N_i/\Phi_{eq}$ for the individual radiation-produced states.

Typical total radiation-induced introduction rates from microscopic measurements are $(1-10)$ cm$^{-1}$ (Ref. [4,10]). Using the value $\alpha_{irr}/\Phi_{eq} = 3 \times 10^{-16}$ cm from Fig. 5 gives a range for the average $\sigma$ of $(3 - 0.3) \times 10^{-16}$ cm$^2$, which is similar to the electron/hole cross-sections obtained from the microscopic measurements. It is also noted that the measured $\sum_i (\beta_i \cdot \sigma_i(\lambda))$ decreases with increasing $\lambda$. The interpretation is, that due to energy conservation, the fraction of the band-gap which can be reached by electrons from the valence band increases with photon energy. A similar argument holds for holes.

The light absorption for photons with energies close to the band-gap energy, $E_{gap}$, is sensitive to the value of $E_{gap}$. Whereas the dependence of $E_{gap}$ on the dopant density, $N_d$, in silicon has been studied in detail [11–13], there are hardly any results on its dependence after irradiation. $E_{gap}$ is observed to decrease with $N_d$, however the change is less than $\approx 5$ meV for $N_d < 10^{17}$ cm$^{-3}$. According to Refs. [14–16] the dependence of the absorption coefficient for a semiconductor with an indirect band gap can be approximated by $\alpha \propto (E_\gamma - E_{gap} + E_{ex} \pm \hbar\omega_p)^2$ for photon energies $E_\gamma > E_{gap} + \hbar\omega_p$. The phonon energy required for energy and momentum conservation is $\hbar\omega_p$. The + sign refers to phonon absorption and the − sign to phonon emission. $E_{ex}$ is the exciton binding energy which describes the interaction of the generated electron–hole pair. Assuming $E_{ex}$ and $\hbar\omega_p$ do not change with irradiation the intercept of a straight-line fit to the linear part of $\sqrt{1/\lambda_{abs}}(E_\gamma)$ with $\sqrt{1/\lambda_{abs}}(E_\gamma = E_g) = 0$ should give $E_g - E_{gap} = const$ similar to Ref. [11]. Methods to determine $E_{gap}$ directly are described in Refs. [15,17] but were not applicable to our data due to the rather large step size of $\Delta\lambda = 1$ nm.

Fig. 6 shows $\sqrt{1/\lambda_{abs}}$ as a function of the photon energy, $E_\gamma$, for the different $\Phi_{eq}$ values. For $E_\gamma \gtrsim 1.18$ eV the dependence is linear. The intercept of straight-line fits in the range $E_\gamma = 1.2$–1.3 eV with $\sqrt{1/\lambda_{abs}} = 0$ is $E_g(\Phi_{eq})$. For $\Phi_{eq} = 0$ the value $E_g(0) = (1.1230 \times 10^3 \, {}^{+1.0}_{-0.4} \pm 2.0 \pm 0.5)$ meV is found. The first uncertainty is obtained by changing the fit range by $\pm 20$ meV, the second by changing the $\lambda$ scale of the spectrophotometer by $\pm 2$ nm, and the third by calculating the change of $E_{gap}$ for a temperature change by $\pm 2$ °C, using the temperature dependence of $E_{gap}$ of $-0.25$ meV/°C at $+20$ °C from Ref. [18]. The systematic effect of a possible local variation of the $\lambda$ scale is not taken into account. The statistical uncertainty of the extrapolation is
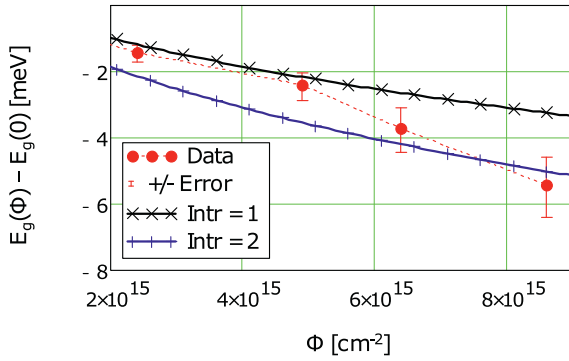
**Fig. 7.** Difference $E_g(\Phi) - E_g(0)$ obtained from the extrapolation of the straight-line fits shown in Fig. 6. As discussed in the text the difference is to a good approximation equal to $\Delta E_{gap}(\Phi_{eq})$, the change of the silicon band-gap with irradiation. The two curves are obtained by using Eq. (6) assuming $N_d = Intr \cdot \Phi_{eq}$ for the two values $Intr = 1$ and $2$ cm$^{-1}$.

negligible. The value of $E_{gap}$ from Ref. [18] is $E_{gap} = 1.126$ eV with an estimated uncertainty of 1 meV. The observed difference is $E_g - E_{gap}$ is $-3^{+4}_{-5}$ meV.

Fig. 7 shows the difference $E_g(\Phi_{eq}) - E_g(0)$ as a function of $\Phi_{eq}$. The error bars take into account that most of the uncertainties of the $E_g$ determination for the different $\Phi_{eq}$ values are correlated and cancel in the difference. Also most of the model uncertainties are expected to cancel in the difference. Assuming that $E_{ex}$ and $\hbar\omega_p$ do not change with irradiation, the change of the silicon band-gap with fluence is $\Delta E_{gap}(\Phi_{eq}) = E_g(\Phi_{eq}) - E_g(0)$. The data shown in Fig. 7 suggest that $\Delta E_{gap}(\Phi_{eq}) \propto \Phi_{eq}$.

In Ref. [13] the following parametrization for $\Delta E_{gap}$ as a function of doping $N_d$ is given:

$$\Delta E_{gap}(N_d) = A \cdot \left( \ln(N_d/N_{ref}) \right)^b . \tag{6}$$

The value of $A$ for $n$-type silicon is $(3.67 \pm 0.20) \times 10^{-5}$ eV if Boltzmann statistics is assumed, and $(4.20 \pm 0.30) \times 10^{-5}$ eV for Fermi–Dirac statistics. The parameter $N_{ref} = 10^{14}$ cm$^{-3}$, and the exponent $b = 3$. To relate the fluence $\Phi_{eq}$ to the number of states, an introduction rate has to be assumed. The curves in Fig. 7 correspond to introduction rates of 1 cm$^{-1}$ and 2 cm$^{-1}$, respectively, assuming the parameters for Boltzmann statistics. The values of $\Delta E_{gap}$ for data and model are similar, however the assumption of an introduction rate of 1 to 2 cm$^{-1}$ for damage states which introduce a band gap shift, is completely ad hoc. It is also not clear, if Eq. (6) can be extrapolated to such low concentrations of charged defects. In Ref. [19] a linear dependence of $\Delta E_{gap}$ on neutron irradiation fluence with a value $\Delta E_{gap}/\Phi = -2 \times 10^{-18}$ eV·cm$^2$ is reported. For the maximal fluence of the absorption measurement of this paper, $\Phi_{eq} = 8.6 \times 10^{15}$ cm$^{-2}$, the expected value for the band-gap shift would be $\Delta E_{gap} = -17$ meV, significantly larger than what is observed, assuming a hardness factor of 1 for the irradiations of Ref. [19]. Additional work is required to clarify the situation.

It should also be noted that most of the damage by 24 GeV/c protons results in defect clusters, whereas the dopants are atoms located at the lattice points. Ref. [20] proposes that cluster defects can change the potential locally, which results in a local change of the band gap. In Ref. [21] it is shown that the activation energy of states in clusters can be several meV lower than for point defects. Such effects can possibly explain the $\Phi_{eq}$-dependence and the magnitude of $\Delta E_{gap}$.

## 6. Conclusions and outlook

The change of the light-absorption length in silicon, $\lambda_{abs}(\Phi_{eq}, \lambda)$, due to radiation damage by 24 GeV/c protons for 1 MeV neutron-equivalent fluences, $\Phi_{eq}$, up to $8.6 \times 10^{15}$ cm$^{-2}$ has been measured using

a spectrophotometer. The measurements were performed at +20 °C for wavelengths, $\lambda$, between 0.95 and 1.30 μm. In the $\Phi_{eq}$-range investigated it is found that $\alpha_{irr}(\Phi_{eq}, \lambda) = 1/\lambda_{abs}(\Phi_{eq}, \lambda) - 1/\lambda_{abs}(0, \lambda)$ is proportional to $\Phi_{eq}$. A phenomenological parametrization of $\alpha_{irr}(\lambda)/\Phi_{eq}$ is presented, which, together with the $\lambda_{abs}(0)$ data for non-irradiated silicon of Ref. [6,7], allows to calculate $\lambda_{abs}(\Phi_{eq}, \lambda)$. Edge-TCT measurements of strip sensors irradiated to $\Phi_{eq} = 9.4 \times 10^{15}$ cm$^{-2}$ performed at $-30$ °C with light of $\lambda = 1.052$ μm confirm the observed decrease of $\lambda_{abs}$ with $\Phi_{eq}$. The quantity $\alpha_{irr}/\Phi_{eq}$ is interpreted as $\sum_i (\beta_i \cdot \sigma_i(E_\gamma))$, the sum over the products of the introduction rates of the radiation-induced damage states $\beta_i$ times the corresponding photon cross-sections $\sigma_i(E_\gamma)$.

From the measured $\lambda_{abs}(\Phi_{eq}, \lambda)$ the change of the band-gap energy, $\Delta E_{gap}(\Phi_{eq})$, as a function of $\Phi_{eq}$ is extracted. $\Delta E_{gap}(\Phi_{eq})$ is approximately proportional to $\Phi_{eq}$ and reaches a value of $\approx -5$ meV at the highest fluence of $\Phi_{eq} = 8.6 \times 10^{15}$ cm$^{-2}$.

The measurements and results presented are a step towards a systematic study of the radiation-induced change of light absorption in silicon. A next step could be to determine $\alpha_{irr}$ as a function of temperature using spectrophotometer measurements. With edge-TCT $\alpha_{irr}$ can be studied as a function of temperature, electric field and current. These parameters influence the occupancy of the radiation-induced states and therefore the photon cross-sections $\sigma_i$.

As the $\sigma_i(E_\gamma)$ times the densities of damage centers, $N_i$, enter into the calculation of the specific energy loss of charged particles, d$E$/d$x$ [22,23], the generation of charge carriers per unit length may be different for non-irradiated and irradiated sensors. However, the expected effect is estimated to be negligibly small. For the band-gap narrowing due to radiation damage further studies are required to verify the results presented in this paper and refine the analysis methods.

## Declaration of competing interest

The authors declare that they have no known competing financial interests or personal relationships that could have appeared to influence the work reported in this paper.

## CRediT authorship contribution statement

**C. Scharf:** Conceptualization, Investigation, Methodology, Writing - review & editing. **F. Feindt:** Investigation, Methodology. **R. Klanner:** Validation, Methodology, Writing - review & editing.

## Acknowledgments

## References

[1] H. Fan, A. Ramdas, Infrared absorption and photoconductivity in irradiated silicon, J. Appl. Phys. 30 (8) (1959) 1127–1134.

[2] C. Scharf, Radiation Damage of Highly Irradiated Silicon Sensors (Ph.D. thesis), Hamburg University, 2018, http://dx.doi.org/10.3204/PUBDV-2018-03707, PUBDV-2018-03707.

[3] F. Feindt, Edge-TCT for the Investigation of Radiation Damaged Silicon Strip Sensors (M.Sc. thesis), Hamburg University, 2017, DESY-THESIS-2017-006.

[4] M. Moll, et al., Relation between microscopic effects and macroscopic changes in silicon detector properties after hadron irradiation, Nucl. Instrum. Methods Phys. Res. 186 (2002) 100–110.

[5] www.agilent.com.

[6] M.A. Green, M.J. Keevers, Optical properties of intrinsic silicon at 300 K, Prog. Photovolt., Res. Appl. 3 (1995) 189–192, data accessible at www.pveducation. org/pvcdrom/materials/optical-properties-of-silicon.

[7] M.A. Green, Self-consistent optical parameters of intrinsic silicon at 300 K including temperature coefficients, Sol. Energy Mater. Sol. Cells 92 (2008) 1305–1310.

[8] G. Kramberger, et al., Investigation of irradiated silicon detectors by edge-TCT, IEEE Trans. Nucl. Sci. 57 (4) (2010) 2294–2302.

[9] G. Kramberger, et al., Modeling of electric field in silicon micro-strip detectors irradiated with neutrons and pions, JINST 9 (2014) P10016.

[10] G. Davies, et al., Radiation damage in silicon exposed to high-energy protons, Phys. Rev. B 73 (2006) 165202, 1–10.

[11] S.E. Aw, H.S. Tan, C.K. Ong, Optical absorption measurements of band-gap shrinkage in moderately and heavily doped silicon, J. Phys.: Condens. Matter 3 (1991) 8213–8223.

[12] P.P. Altermatt, et al., Reassessment of the intrinsic carrier density in silicon in view of band-gap narrowing, J. Appl. Phys. 93 (3) (2003) 1598–1604.

[13] Di Yan, A. Cuevas, Empirical determination of the energy band-gap narrowing in p$^+$ silicon heavily doped with boron, J. Appl. Phys. 116 (2014) 194505, 1–7.

[14] R.J. Elliott, Intensity of optical absorption by excitons, Phys. Rev. 108 (6) (1957) 1384–1389.

[15] G.G. Macfarlane, T.P. McLean, J.E. Quarrington, Fine structure in the absorption-edge spectrum of Si, Phys. Rev. 111 (5) (1958) 1245–1254.

[16] P.Y. Yu, M. Cardona, Fundamentals of Semiconductors: Physics and Materials Properties, Springer, Berlin/Heidelberg, 2010.

[17] W. Bludau, A. Onton, W. Heinke, Temperature dependence of the band gap of silicon, J. Appl. Phys. 45 (4) (1974) 1846–1848.

[18] R. Paessler, Dispersion-related description of temperature dependencies of band gaps in semiconductors, Phys. Rev. B 66 (2002) 085201, 1–18.

[19] H.Y. Fan, Infra-red absorption in semiconductors, Rep. Progr. Phys. 19 (1956) 107–154.

[20] B.R. Gossick, Disordered regions in semiconductors bombarded by fast neutrons, J. Appl. Phys. 30 (8) (1959) 1214–1218.

[21] E.M. Donegani, et al., Study of point and cluster defects in radiation-damaged silicon, Nucl. Instrum. Methods Phys. Res. A 898 (2018) 15–23.

[22] H. Bichsel, Straggling in thin silicon detectors, Rev. Modern Phys. 60 (3) (1998) 663–699.

[23] H. Bichsel, A method to improve tracking and particle identification in TPCs and silicon detectors, Nucl. Instrum. Methods Phys. Res. A 562 (2006) 154–197.